

Theoretical study of the scattering efficiency of rutile titanium dioxide pigments as a function of their spatial dispersion

Jean-Claude Auger, Vincent Arnaud Martinez,
Brian Stout

© FSCT and OCCA 2008

Abstract We propose an original theoretical framework to model the scattering efficiency of white paint films as a function of the volume fraction and spatial state of dispersion of rutile titanium dioxide pigments, taking into account electromagnetic couplings. Numerical calculations are performed using a multiple T matrix formalism on an “elemental” volume extracted from the bulk of the paint and which we model as pigments and fillers in a polymer matrix. Qualitative studies show that, due to the dependent scattering phenomenon, the size of fillers can modulate the magnitude of loss in scattering efficiency by modifying the spatial state of dispersion of the pigments in the polymer matrix. In particular, fillers whose size is comparable to the dimension of the pigments improve the scattering efficiency by impeding crowding. It is also shown that the optical properties of the bulk material at arbitrary concentration can be approximated by extrapolating the optical properties calculated on a limited number of scatterers.

Keywords Optical property, Opacity, Rutile titanium dioxide pigment, Dependent scattering, Multiple scattering, Spatial dispersion, T-matrix formalism

J.-C. Auger (✉)

Center for Laser Diagnostics, Department of Applied Physics, Yale University, New Haven, CT 06520, USA
e-mail: jeanclaude_auger@hotmail.com

V. A. Martinez

Department of Applied Physics, RMIT University, Melbourne, VIC 3000, Australia

B. Stout

Institut Fresnel, UMR 6133, Faculté des Sciences et Techniques, Centre de Saint Jérôme, Marseilles Cedex 20 13397, France

Introduction

The opacity of architectural white paint films is due to the multiple scattering interactions that occur between the incident radiation and small particles dispersed in the polymer matrix. Total covering is achieved when all the photons penetrating the paint undergo a sufficient number of scattering processes to be scattered back into the incident media before they can be reflected or absorbed by the substrate or absorbed within the film. The strength of the single scattering phenomena is directly related to the contrast between the index of refraction of the pigments and the index of refraction of the surrounding medium. The larger the contrast, the stronger is the amplitude of the scattering events. For this reason, rutile titanium dioxide (TiO_2) with an index refraction of ~ 2.8 and negligible absorption in the visible range is an efficient pigment for use in white coatings.

Now, if the existence of a nonnegligible refraction index contrast of the particles with the surrounding medium is the sine qua non condition to generate scattering, there also exists a wide range of other parameters that can modulate its strength and efficiency. Such parameters can be classified as either intrinsic or extrinsic with respect to the pigments. The intrinsic category refers to the chemical nature, size, and shape of the pigments while extrinsic parameters include the filling fractions and the spatial dispersion state of the pigments in the polymer matrix. Through the years, paint manufacturers have realized numerous studies to increase the effectiveness of TiO_2 ^{1,2} by optimizing each of these variables. One major result of this optimization is that many commercial TiO_2 grades now have their size distribution as narrow as technically possible and centered about $0.250 \mu\text{m}$ in diameter to maximize scattering.

A major issue under constant investigation is the minimization of the loss in scattering efficiency due to

the pigment packing that unavoidably arises in highly concentrated paints. This decrease in light scattering effectiveness is attributed to the occurrence of dependent light scattering phenomena^{3,4} and is known to cause significant increase in the cost of the manufacture of paints. Indeed, the higher is the filling fraction; the larger the amount of TiO₂ pigments that must be added to the formulation to reach a nonnegligible enhancement of the overall paint opacity. Semiempirical studies have shown that this undesirable phenomenon can be attenuated by improving the spatial dispersion and limiting the aggregation states of the pigments in the dry film.^{5–7} To our knowledge, few studies^{7,8} propose the analysis of this intricate problem through a theoretical framework that takes into account exact dependent light scattering calculations.

Consequently, the aim of this work is twofold: first, to propose an original approach that allows studying the complex relation between the spatial state of dispersion of rutile TiO₂ pigments and their scattering efficiency; and second, to discuss the effects of such relation on the opacity of the global paint film. Our framework consists in calculating and comparing the optical properties related to elemental volumes of different paints under study. The multiple scattering T matrix formalism⁹ is described in the next section. In the second section, the formalism is applied to study the variations of the optical properties of TiO₂ pigments randomly and uniformly dispersed in a polymer matrix as a function of the filling fractions. Finally, the last section treats the analysis of the changes in the optical properties when the spatial dispersion of the pigments is altered by taking into account the presence of fillers.

Theoretical framework

Modeling the dry paint films

White, water-based coatings are complex systems, primarily composed of “opaque” pigments (most commonly rutile titanium dioxide), fillers, dispersants, rheology modifiers, and a latex binder. From the optical point of view, the pigments are the only elements that efficiently scatter light and thereby contribute to the opacity. Rheology modifiers and dispersants are in too small proportions to be relevant while most of the fillers, such as clays, have refraction indices ranging from 1.5 to 1.7, and have an index contrast too small to effectively contribute to the scattering efficiency. Nevertheless, the fillers whose sizes vary from half to about tens of microns can indirectly modify the optical properties by altering the spatial distribution of the pigments in the dry film. Thus, considering bulk properties and disregarding the interfaces, white paints can be modeled as a binary mixture composed of TiO₂ pigments and fillers dispersed in a continuous polymer matrix at the volumetric concentrations f_p and f_c ,

respectively. Our approach consists in calculating the optical properties of an elemental of volume element, V_0 , extracted from the bulk material, and to comprehensively take into account both multiple and dependent scattering phenomena. To simplify the theoretical description, it is assumed that the pigments and the fillers have spherical shapes and constant radii, denoted r_p and r_c , respectively. Furthermore, the elemental cell V_0 , containing N_p pigments and N_c fillers, is assumed to be spherical.

Multiple T matrix formalism

The incident radiation upon the cell is taken to be a monochromatic plane wave, characterized by its vacuum wavelength, λ_0 , and its in-medium wave vector, \mathbf{K}_{inc} , such that $|\mathbf{K}_{\text{inc}}| = 2\pi n_0/\lambda_0$ where n_0 is the real index of refraction of the embedding medium. The positions of the pigments, of complex refraction index contrast, $\tilde{n}_p \equiv n_p/n_0$, are given in terms of position vectors $\mathbf{R}^{(i)}$ ($i = 1, \dots, N_p = N$) defined with respect to a main reference frame noted \mathfrak{R}_0 . Combining the multiple scattering equation of light and the superposition principle of electromagnetic theory, the exciting electric field upon the i th scatterer ($\mathbf{E}_{\text{exc}}^{(i)}$) can be expressed as the sum of the applied incident electric radiation (\mathbf{E}_{inc}) and the scattered fields of all the remaining particles ($\mathbf{E}_s^{(j)}$) such that:

$$\mathbf{E}_{\text{exc}}^{(i)} = \mathbf{E}_{\text{inc}} + \sum_{\substack{j=1 \\ j \neq i}}^N \mathbf{E}_s^{(j)} \quad i = 1, \dots, N \quad (1.1)$$

The multiple scattering T matrix formalism has already proved to be an effective approach to solving the linear system of couple equations defined in (1.1).¹⁰ Assuming that the incident, scattered, and internal electromagnetic fields are expanded on the spherical vector wave functions, the multiple-scattering T -matrices can be re-written such that they satisfy the equations:

$$\overline{\mathbf{T}}_N^{(i)} = \overline{\mathbf{T}}_1^{(i)} \left[\overline{\mathbf{I}} + \sum_{\substack{j=1 \\ j \neq i}}^N \overline{\mathbf{H}}^{(i,j)} \overline{\mathbf{T}}_N^{(j)} \overline{\mathbf{J}}^{(j,i)} \right] \quad i = 1, \dots, N \quad (1.2)$$

The $\overline{\mathbf{J}}^{(i,j)}$ and $\overline{\mathbf{H}}^{(i,j)}$ are matrices¹¹ which translate the incident and scattered fields, respectively, from a reference frame centered on the j th particle to a reference frame centered on the i th particle. The $\overline{\mathbf{T}}_1^{(i)}$ represents the single-particle T matrix of the i th object,¹² which relates the expansion coefficients of the excitation field impinging on the particle into the expansion coefficients of the field radiated by the particle. Finally, the $\overline{\mathbf{T}}_N^{(i)}$ symbolizes the N -particle T matrix of the i th objects. The $\overline{\mathbf{T}}_N^{(i)}$ directly relates the

scattered field to the expansion coefficients the field incident on the system while taking into account the presence of all the other particles in the system. It is independent of the orientation or polarization of the incident wave and it characterizes the scattering properties of the particle while taking into account the presence of the others. Once the N -particle T matrices are calculated by solving (1.2), the optical properties of the whole system can be easily determined for arbitrary incident fields.¹³ In this study, numerical simulations were performed with the Recursive Centered T Matrix Algorithm (RCTMA), whose thorough description and validation have already been presented in the literature.¹⁴

The number of particles that can be handled in the calculations is largely limited by the size parameter (defined as $|\mathbf{K}_{\text{inc}}|r_p$) of the primary particles, which plays a dominant role in determining the number of multiple components necessary to describe the interactions. The larger the dimension of the particles with respect to the wavelength of the incident radiation, the larger the number of partial waves that must be taken into account to accurately represent the electric fields expansions on the spherical wave basis and consequently the higher are the computational resources required to achieve reliable calculations.

Construction of the cell

An essential aspect of our framework is to generate the position vectors $\mathbf{R}^{(i)}$ such that the spatial distribution of the scatterers within the cell can reasonably approximate an elemental volume of the modeled paint under study. To fulfill this requirement, we apply the following procedure: (a) the volume of the cell V_0 is calculated from the knowledge of N_p , f_p , and r_p , (b) the radius of the fillers r_c is deduced from f_c , N_c , and V_0 , (c) the Cartesian coordinates, $x^{(i)}$, $y^{(i)}$, and $z^{(i)}$ related to the i th position vector (of both pigments and fillers) which are randomly generated from a uniform distribution function and accepted provided that each added particle is entirely confined within V_0 and that its volume does not overlap with any previously placed objects in the cell. When present, the fillers were systematically placed in the cell before the pigments.

Numerical calculations and statistical treatment

Taking \mathbf{K}_{inc} to be parallel to the Oz axis of the main reference frame, the RCTMA is applied at each configuration, labeled by k , to compute the scattering cross sections $C_s^{(k,p)}$ and asymmetry parameter $g^{(k,p)}$ of the cell, where $p = 1, 2$ correspond, respectively, to two orthogonal linear polarizations of the incident radiation. The expressions of the configuration and polarization average scattering cross section and scattering efficiency are calculated from:

$$\langle C_s \rangle_N^K \equiv \frac{1}{2K} \sum_{k=1}^K \sum_{p=1}^2 C_s^{(k,p)} \quad (1.3)$$

$$\langle s \rangle_N^K \equiv \frac{1}{2K} \sum_{k=1}^K \sum_{p=1}^2 C_s^{(k,p)} (1 - g^{(k,p)}) \quad (1.4)$$

where N , f_p , and r_p are fixed, K is the total number of configurations, $\langle \rangle_N^K$ stands for configuration and polarization average operating. The corresponding optical properties per unit pigment volume are simply given by $\langle C_s^V \rangle_N^K \equiv \langle C_s \rangle_N^K / Nv_p$ and $\langle S \rangle_N^K \equiv \langle s \rangle_N^K / Nv_p$ where v_p is the volume of a single pigment. We believe that this statistical approach is a nonnegligible improvement compared to previous works^{15,16} that proposed the modulation of couplings between the objects by translating the particles along the different axes of a Cartesian coordinate system.

Finally, it must be mentioned that multiple T matrix formalism allows direct analytical formulations of the orientation and polarization average scattering cross section ($C_s^{(k)}$) (as well as the asymmetry parameter $g^{(k)}$) with respect to the incident radiation. Such formulations provide an alternative scheme to evaluate $\langle C_s \rangle_N^K$ and $\langle s \rangle_N^K$, which in principle should involve fewer configurations to converge to the same level of precision. Nevertheless, in addition to the complexity of the analytical formulations that must be programmed, this approach has the disadvantage of requiring the evaluation of numerous translational matrices, entailing considerable amount of CPU time.

Application to the study of the optical properties of randomly dispersed TiO₂ pigments

Description of the systems

The aim of this section is to apply our method to study the variations of the configuration average scattering cross section and scattering efficiency of various ensembles of titanium dioxide pigments randomly dispersed in a polymer resin (see Fig. 1a). Henceforth, the subscripts (superscripts) N and K are omitted for the sake of clarity. Calculations were performed as functions of the filling fraction and the number of particles such that $f_p = 0.01, 0.05, 0.10, 0.15, 0.20$ and $N_p = 1, 3, 4, 5, 6, 9, 12, 15, 18, 21, \text{ and } 30$. In a previous work¹⁷ we have found that decreasing K from 3000 to 1000 and then to 200 led to changes in $\langle C_s \rangle$ from about 1% to a few percent, respectively. Therefore, we adopted $K = 1000$ except in the cells containing 30 particles where, as a result of the extensive computation times involved, K , the number of configurations was limited to 200. The wavelength of the incident radiation was fixed at 0.546 μm , which corresponds to the middle of the visible range and the corresponding

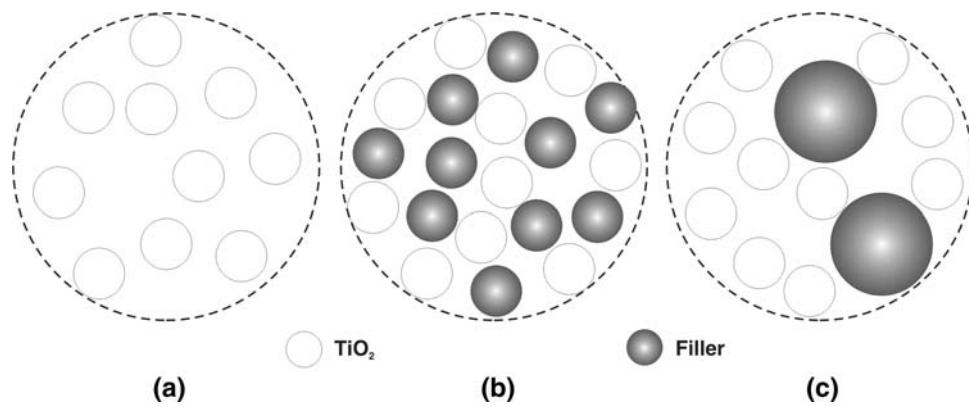


Fig. 1: Representation of the cells under study. (a) Randomly dispersed pigments without fillers. (b) Randomly dispersed pigments and fillers having identical sizes. (c) Randomly dispersed pigments and fillers having different sizes

indices of refraction for the rutile titanium and the polymer matrix were set to 2.8 and 1.5, respectively. The radius of the TiO_2 particles was fixed to $0.132 \mu\text{m}$, which reasonably approximate the maximum of the particle size distribution of common titanium dioxide pigments available on the market. The variations of $\langle C_s \rangle$ and $\langle s \rangle$ as a function of the number of particles in the cell and for the different filling fractions are displayed in Figs. 2a and 2b. The bold lines correspond to the optical properties of the cell obtained from independent single particle scattering calculations, henceforth referred to as C_{ind} and s_{ind} , respectively. These quantities are useful to quantify the magnitude of the electromagnetic couplings by, respectively, evaluating the ratios $\langle C_s \rangle / C_{\text{ind}}$ and $\langle s \rangle / s_{\text{ind}}$.

Effect of the number of particles in the cell

Inspection of Figs. 2a and 2b shows that independently of the concentration, the scattering cross sections and scattering efficiencies monotonously increase as functions of the number of particles in the cells. This upward trend is readily understood by recalling that multiple T-matrix formalism assumes that the incident radiation is a monochromatic plane wave with an infinite spatial extension. Thereby, as the size of the cell increases along with the number of particles, the interaction front with the incident wave is enlarged and the scattering cross section is enhanced. The monotonous character of the rise is due to the configuration averaging process that makes $\langle C_s \rangle$ and $\langle s \rangle$ intrinsic properties of the system that do not depend on the relative positions between the scatterers but rather on an average distance, which is only function of the filling fraction. Therefore, any resonant modes that could be associated with a specific arrangement of the particles and which could lead to possible oscillations in the variations of the optical parameters when increasing the number of particles from N to $N + 1$ are canceled out. A further significant feature is that the statistical variations of $\langle C_s \rangle$ and $\langle s \rangle$ for the different filling

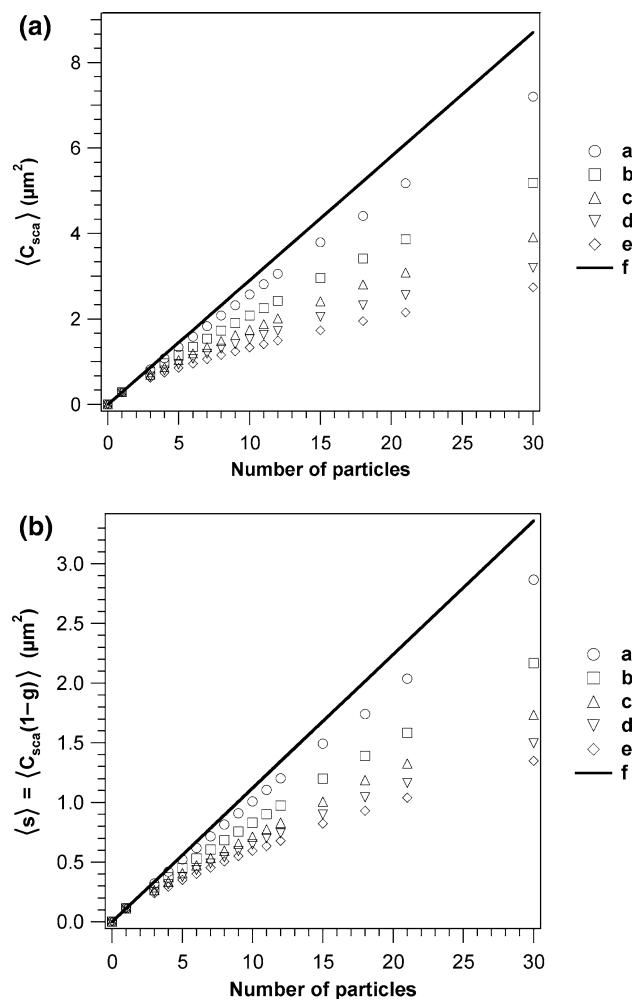


Fig. 2: (a) Configuration average scattering cross section as function of the number of particles in the cell for no fillers (Fig. 1a). (a) $f_p = 0.01$, (b) $f_p = 0.05$, (c) $f_p = 0.10$, (d) $f_p = 0.15$, (e) $f_p = 0.20$, (f) Independent scattering approximation. (b) Configuration average scattering efficiency as function of the number of particles in the cell for no fillers (Fig. 1a). (a) $f_p = 0.01$, (b) $f_p = 0.05$, (c) $f_p = 0.10$, (d) $f_p = 0.15$, (e) $f_p = 0.20$, (f) Independent scattering approximation

fractions do not overlap with other. Therefore, one can assert that the conclusions of qualitative comparisons between different systems with different concentrations are independent of the number of particles in the cell.

Effect of the filling fraction

Inspection of Figs. 2a and 2b clearly exhibits that at a constant number of particles, the difference between $\langle C_s \rangle$ and $\langle C_{ind} \rangle$ (respectively, $\langle s \rangle$ and s_{ind}) is enhanced when the pigment filling fraction is increased. This gradual loss in scattering effectiveness is due to the strengthening of the near field electromagnetic interactions when the average distance between the scatterers decreases within the cell.

In addition, a comparative analysis between the relative variations of both optical parameters shows that the effect of dependent scattering seems to be more pronounced on the scattering cross sections than on the scattering efficiencies. For example, the ratios $\langle C_s \rangle / C_{ind}$ and $\langle s \rangle / s_{ind}$ of the cell composed by 30 particles at $f_p = 0.2$ are, respectively, about 0.3 and 0.4. This tendency can be understood by considering that if an increase in the filling fraction effectively enhances the dependent scattering and thereby decreases the scattering per particle, this effect is partially counterbalanced by an enhancement in backscattering.

Extrapolation of the optical properties to large number of scatterers and continuous range of concentrations

As was previously established, the restriction to relatively low numbers of particles in the cell, imposed by realistic computation resources, does not affect the reliability of qualitative analysis. Nevertheless, it does currently prevent calculations on systems composed by hundreds of scatterers that could provide a reasonable estimation of the optical properties of the bulk material. Therefore, we now focus on the possible extrapolation of the optical properties of cells composed by very large numbers of particles from the optical properties of relatively small ensemble of scatterers. This analysis is carried out in terms of $\langle C_s^V \rangle \equiv \langle C_s \rangle / N v_p$ rather than $\langle C_s \rangle$; it is a more relevant parameter in light scattering analysis (as can be remarked by its units, length^{-1}).

The variations of $\langle C_s^V \rangle$, evaluated from the data set presented in Fig. 2a, are plotted in Fig. 3 as a function of the number of particles. The horizontal line represents the scattering cross section per unit volume (C_{ind}^V) calculated using the independent scattering approximation. It can be seen that for each filling fraction, the orientation averaged scattering cross sections exhibits a monotonous decrease as a function of particle number characterized by a rapid drop followed by a pseudo asymptotic plateau. We also remark that due to

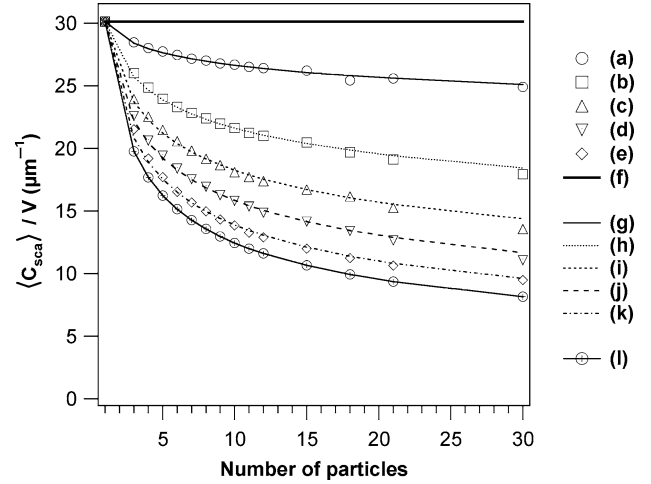


Fig. 3: Configuration average scattering cross section by unit volume as function of the number of particles in the cell (no fillers Fig. 1a). (a) $f_p = 0.01$, (b) $f_p = 0.05$, (c) $f_p = 0.10$, (d) $f_p = 0.15$, (e) $f_p = 0.20$, (f) Independent scattering approximation, (g) fit $f_p = 0.01$, (h) fit $f_p = 0.05$, (i) fit $f_p = 0.10$, (j) fit $f_p = 0.15$, (k) fit $f_p = 0.20$, (l) interpolation $f_p = 0.25$

dependent scattering effects, the higher the filling fraction, the stronger the descent, and the larger the number of particles in the system, denoted N^* , necessary to reach the “plateau”. Each data set were readily fitted using a power law function, which in general form is given by:

$$\langle C_s^V \rangle(N, f_p) = \gamma + \beta N^\alpha \quad (1.5)$$

Taking into account that $\langle C_s^V \rangle(f_p, N = 1) = C_{ind}^V$, allows us to set:

$$\begin{cases} \gamma = 0 \\ \beta = C_{ind}^V \\ \alpha = \alpha(f_p) \end{cases} \quad (1.6)$$

In view of the poor statistics in the evaluation of the configuration average scattering cross section of systems composed of 30 particles, the fits were performed using the initial data set up to $N_p = 21$. Since this framework implies that at a given filling fraction N is fixed and V_0 is adjusted such that $V_0 = N v_p / f_p$, the condition $f_p \rightarrow 0$ implies $V_0 \rightarrow \infty$ and $\langle C_s^V \rangle = C_{ind}^V$. Combining this last remark with the fact that the variation of $\ln(\alpha)$ plotted as function of $\ln(f_p)$ was perfectly linear (see Fig. 4), relation (1.5) could finally be expressed as:

$$\langle C_s^V \rangle(N, f_p) = C_{ind}^V N^{-\alpha_0 f_p^{\alpha_1}} \quad (1.7)$$

where α_0 and α_1 were found equal to 0.89 and 0.61, respectively.

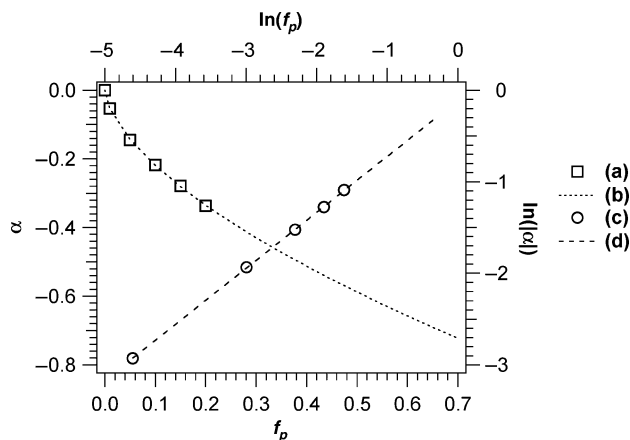


Fig. 4: (a, b) Raw data and corresponding adjustment of $\alpha = \alpha(f_p)$ (left and bottom axis). (c, d) Raw data and corresponding adjustment of $\ln(|\alpha|) = \ln(f_p)$ (right and top axis)

The accuracy of the adjustments obtained from equation 1.7, superimpose on the original set of data in Fig. 3, shows that: (a) It seems possible to extrapolate the optical properties of cells containing large number of scatterers in a wide range of filling fractions from the knowledge of the optical properties of cell made by relatively small number of particles. (b) The loss in scattering efficiency, represented by the ratio $\langle C_s^V \rangle / C_{ind}^V$, only depends on the two parameters α_0 and α_1 , which are functions of the intrinsic properties n_p , r_p , and n_0 as well as the probability function for each point of space to be occupied by a scatterer. (c) Accurate extrapolations of $\langle C_s^V \rangle$ to large number of particles and high filling fractions rely on the precise determinations of α_0 and α_1 . In principle, such determinations require a prior series of calculations on large ensemble of particles until at least $N \rightarrow N^*$ in a large range of filling fractions. Nonetheless, the linear variation of $\ln(\alpha)$ plotted as a function of $\ln(f_p)$ suggests that the calculations could be limited to two different low concentrations. (d) As a consequence of the previous statement, extrapolation of $\langle C_s^V \rangle$ to the entire range of concentration can be accurately performed. An example is given in Fig. 3, which displays the variation of $\langle C_s^V \rangle$ as a function of N calculated from equation 1.7 setting f_p to 0.25. It is important to point out that the variation of the average scattering cross section given in equation 1.7 by a double power law is consistent with the relation proposed by Hottel et al.²¹ obtained from experimental data. Finally, the study in this paper was carried out on $\langle C_s^V \rangle$, but similar analysis can be performed on $\langle S \rangle$.

Effect of the presence of fillers

The aim of this final section is to study the changes in scattering efficiency of the cell when the spatial state of dispersion of the pigment is modified by the

introduction of fillers. To analyze such variations, we compared the scattering efficiencies of two completely differing systems that correspond to a uniform and packed spatial distribution of the pigments. The former situation was obtained by assuming that the pigments and fillers had similar size ($r_p \approx r_c$) while the latter was achieved by using fillers whose size was much larger than the size of the pigments ($r_p \gg r_c$). A comprehensive interpretation of this study requires the knowledge of the concept of optimum scattering efficiency. This concept is introduced in the following section prior to the discussion.

Notion of optimized scattering efficiency

Opacity is generally given in terms of hiding power (HP) of which units are square meters per liter [$m^2 L^{-1}$]. Its description requires introducing the notion of contrast ratio¹⁸ defined as:

$$CR = 100 \frac{R_b^Y}{R_w^Y} = 100 \frac{\int R_b(\lambda) D_{65}(\lambda) y_{10}(\lambda) d\lambda}{\int R_w(\lambda) D_{65}(\lambda) y_{10}(\lambda) d\lambda} \quad (1.8)$$

where R_b and R_w are the reflection coefficients of the paint film measured on, respectively, black and white substrates, y_{10} is the tristimulus function and D_{65} is the illuminant. It is assumed that when the CR reaches 98%, the human eye cannot distinguish any further changes in opacity. Thereby, HP represents the area that a unit volume of wet paint can cover at a film thickness Z sufficient to produce a contrast ratio 98% when the paint has dried. The higher the hiding power, the larger is the area a fixed volume of paint can cover.

Thus, one can define the optimal scattering efficiency, noted S_o , as the scattering efficiency that a paint film must reach to fulfill a giving hiding power without wasting raw materials. This notion can be illustrated with the use of the Kubelka–Munk theory.¹⁹ Within the framework of our example, the theoretical contrast ratios of three hypothetical paints whose scattering efficiencies are 0.25, 0.20, and 0.15 μm^{-1} have been calculated as a function of the film thickness and displayed in Fig. 5. Results show that to reach a hiding power of about 14.2 square meters per liter, corresponding to $Z = 72 \mu m$, the paint's scattering efficiency must be at least superior to 0.20 μm^{-1} . For this same paint thickness, pigments scattering efficiencies of 0.15 and 0.25 μm^{-1} , respectively, lead to contrast ratios of 96.5 and 98.7%. Thus, while the 0.15 μm^{-1} efficiency cannot provide total covering at the required thickness, the 0.25 μm^{-1} efficiency exceeds the constraint, implying a waste of raw materials.

Results and discussion

For the study in this section, the number of pigment was set to 21 while the filling fraction of the fillers is

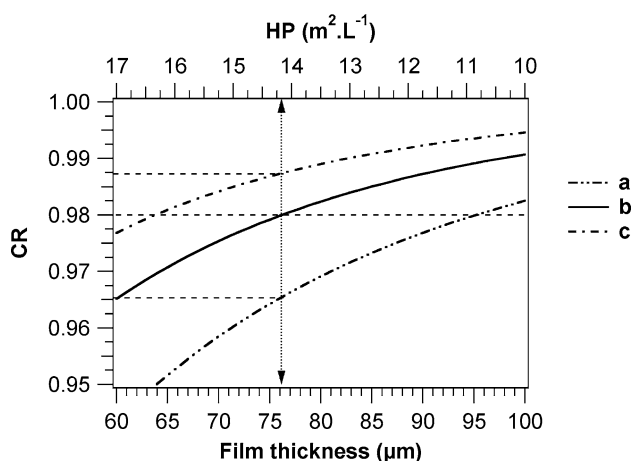


Fig. 5: Variation of the contrast ratio as a function of the film thickness from the Kubelka–Munk theory. (a) $S = 0.25 \mu\text{m}^{-1}$, (b) $S = 0.20 \mu\text{m}^{-1}$, (c) $S = 0.15 \mu\text{m}^{-1}$

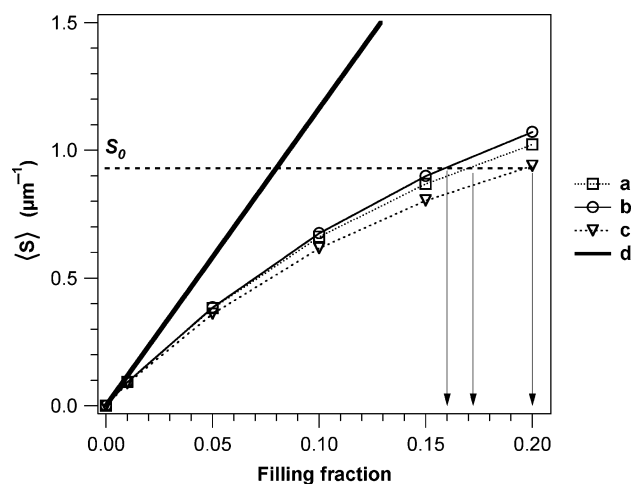


Fig. 6: Variation of the scattering efficiency as a function of the filling fraction corresponding to the following cell: (a) 21 pigments Fig. 1a, (b) 21 pigments and 21 fillers Fig. 1b, (c) 21 pigments and 2 fillers Fig. 1c

kept constant at $f_c = 0.1$. The configuration average scattering efficiency per unit volume is calculated as a function of various filling fractions ($f_p = 0.01, 0.05, 0.10, 0.15,$ and 0.20) considering: (b) $N_c = 21$ and (c) $N_c = 2$ as shown in Figs. 1b and 1c. Results displayed in Fig. 6 illustrate that the loss in scattering efficiency due to dependent scattering phenomena is strongly correlated to the spatial dispersion state of the pigments within the cell. Independent of the filling fraction, the highest scattering efficiency is always reached when the size of the fillers is similar to the size of the pigments (see Fig. 1b) whereas the strongest loss corresponds to the system that promotes crowding (see Fig. 1c). Also, as electromagnetic couplings are amplified in more dense systems, the higher the filling fraction, the larger the differences. Consequently in the range of high filling fractions, variations in the size of the fillers lead to equal scattering efficiencies with different quantities of pigments.

Considering the hiding power that the paint film must attain implies an optimal scattering efficiency around $S_0 = 0.92 \mu\text{m}^{-1}$. Figure 6 shows that such value is attained for f_p equal to 0.20 and 0.16 for the systems (c) and (b), respectively. Thus, within the framework of this illustration, optimizing the spatial dispersion state of the pigments in the paint film allows reaching this S_0 with 4% less titanium dioxide. In practice, the savings in pigment concentration will need to be compared to the extra cost related to the use of smaller fillers and to the modification in mechanical processes of dispersion it can imply during production. Also, in this study, we considered that opacity was the only optical property that needed to be optimized, but it is important to mention that gloss can also be modified by the change in the fillers size distribution.

Finally, for comparison, the scattering efficiency of the cells composed of uniformly dispersed TiO_2 (see Fig. 1a) was also included in Fig. 6. Results show that it

lay in between the two latter systems and that at high filling fraction it is closer to the results given by system (b). Nevertheless, when considering the result obtained on the scattering cross section alone (not shown in the article), it tends to be closer to the value obtained by system (c). One can conclude that direct comparison between systems (a) and systems (b) and (c) should be handled with care. Indeed, one could expect the scattering efficiency of system (a) to be superior to the one given by the TiO_2 pigments mixed with charges of comparable size if the dispersing effect is counterbalanced by the lack of real accessible volume to the pigments. Such differences might come from the random generation process and should be the object of further studies.

Variation of the standard deviation as a function of the concentration

In the previous sections, we have studied the variation of the configuration average scattering efficiencies without mentioning the standard deviation (σ_c) related to those quantities. Nevertheless, the spreads in optical properties are interesting parameters, because they provide additional information on the complex relations between the spatial dispersion of the particles and the electromagnetic couplings. In Fig. 7, we display the variations of σ_c as functions of the filling fractions ($f_p = 0.0001, 0.001, 0.01, 0.05, 0.10, 0.15, 0.20,$ and 0.29) evaluated from the scattering cross sections of a mono dispersed (type Fig. 1b) and poly dispersed ensemble of TiO_2 pigments (type Fig. 1c) with the corresponding pigment radii given in Table 1. The particle sizes were chosen to keep N and the total pigment volume, Nv_p , constant during the calculations.

Table 1: Radii in micrometers of the eight spheres composing systems (a) and (b)

Particle	1	2	3	4	5	6	7	8
(a)	0.110	0.110	0.110	0.110	0.110	0.110	0.110	0.110
(b)	0.138	0.138	0.110	0.110	0.087	0.087	0.087	0.087

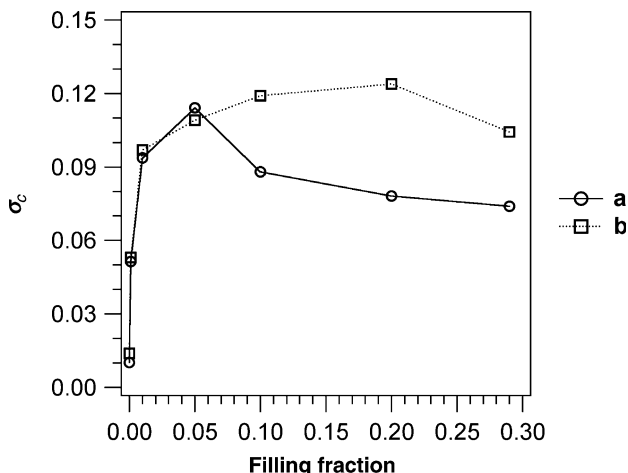


Fig. 7: Standard deviation calculated from the configuration average cross section of eight TiO₂ pigments per cell as a function of the filling fraction. (a) Mono-disperse ensemble of particles (b) Poly-disperse ensemble of particles

One can see that independently of the system, the spreads in cross sections undergo a strong increase from their initial vanishing value, reach a maximum at a given filling fraction noted f_p^m , and then slowly decrease for higher volume fractions. Such variations were mentioned in a previous work,²⁰ can be explained by first considering that in very dilute systems, electromagnetic couplings are negligible and the particles scatter light quasi independently one from the other, therefore $\sigma_c \rightarrow 0$. An increase of the filling fraction amplifies the strength of the electromagnetic couplings and consequently increases the probability of obtaining different values of $\langle C_{sca}^V \rangle$ for each new configuration. As the filling fraction is further increased, the incompressibility of the scatterers leads to the appearance of correlations in the relative positions of the particles. As each point of space does not have the same probability to be occupied, there are less available configurations to the systems and σ_c decreases.

The drop off in σ_c when $f_p > f_p^m$ is much slower than the increasing phase at $f_p < f_p^m$ because even if there are less available configurations to the system, the strength of the coupling is stronger at shorter distances, which increases the probability of having large variations $\langle C_{sca}^V \rangle$ from one configuration to another. A final remark is that at high concentration, σ_c is larger for the poly-disperse system because the number of accessible

configurations is larger than for the mono-disperse system. In principle, when the mono disperse ensemble of spherical particles reaches the maximum compact arrangement ($f_p = 0.72$), there is only one configuration available to the system and $\sigma_c \rightarrow 0$.

Conclusion

We have presented an original theoretical framework permitting the study of the variations of the optical properties of an ensemble of dielectric particles as functions of their spatial state of dispersion in a nonabsorbing medium. We have applied this formalism to compare the loss of scattering efficiencies of various ensembles of TiO₂ pigments with their spatial dispersion states modified by the presence of fillers. The results of our calculations agreed with experimental knowledge, that the opacity of white architectural coatings can be improved using fillers whose sizes are similar to the size of the pigments. This study focused on the opacity of white paint films; however, the framework presented here can be easily applied to the study of dependent absorption that occurs in colored paints by calculating the configuration average absorption cross section of absorbing pigments.

It is clear that such an approach cannot be a substitute for semiempirical and experimental works based on direct measurements of optical properties of paint films in the laboratory. Nevertheless, we believe that the continued development and use of such theoretical frameworks can play a vital role in understanding the fundamental mechanisms that bind the intrinsic and extrinsic properties of the pigments to the opacity or color of paint films.

Finally, we point out that the elemental volume V_0 presented in this framework cannot be easily correlated to the volume element of a heterogeneous medium as introduced in the heuristic derivation of the radiative transfer equation. Indeed, even if this study has shown that one can partially work around the limitations imposed by the truncation of the excited field impinging on each particles by extrapolating the configuration average optical cross sections to larger ensemble of scatterers, two major problems still remain: (a) to determine the size of the cell at which the extrapolation must be performed (b) to accurately extrapolate the phase function of a highly concentrated system, whose knowledge is required to solve the radiative transfer equation.

Acknowledgments The authors would like to thank Eduardo Nahmad for supporting the opening phase of this work and Richard K. Chang for permitting its conclusion.

References

1. Diebold, MP, “Technical Challenges for the TiO₂ Industry.” *JCT CoatingsTech.*, **1** (1) 36–44 (2004)
2. Rutherford, DJ, “Influence of TiO₂ Flocculation on the Optical Properties of Alkyd Emulsion Paints.” *Euro. Coat. J.*, **6** (1) 18–27 (2001)
3. Harding, RH, Golding, B, Morgen, RA, “Optics of Light-Scattering Films. Study of Effects of Pigment Size and Concentration.” *J. Optic. Soc. Am.*, **50** (5) 446–455 (1960)
4. Tunstall, DF, Hird, MJ, “Effect of Particle Crowding on Scattering Power of TiO₂ Pigments.” *J. Paint Technol.*, **46** (588) 33–40 (1974)
5. Braun, JH, “Crowding and Spacing of Titanium Dioxide Pigments.” *J. Paint Technol.*, **60** (758) 67–71 (1988)
6. Stieg, FB Jr, “The Effect of Extenders on the Hiding Power of Titanium Pigments.” *Official Digest*, January, 52–64 (1959)
7. Temperley, J, Westwood, MJ, Hornby, MR, Simpson, LA, “Use of a Mathematical Model to Predict the Effects of Extenders on Pigment Dispersion in Paint Films.” *Pigment Dispers. Paint Film.*, **64** (809) 33–40 (1992)
8. Thiele, ES, French, RH, “Light-Scattering Properties of Representative, Morphological Rutile Titanium Particles Using a Finite-Element Method.” *J. Am. Ceram. Soc.*, **81** (3) 469–479 (1998)
9. McNeil, LE, Hanuska, AR, French, RH, “Orientation Dependence in Near-Field Scattering from TiO₂ Particles.” *Appl. Optic.*, **40** (22) 3726–3736 (2001) doi:10.1364/AO.40.003726
10. Mackowski, DW, Mishchenko, MI, “Calculation of the T Matrix and the Scattering Matrix for Ensembles of Spheres.” *J. Opt. Soc. Am. A*, **13** (11) 2266–2278 (1996)
11. Cruzan, OR, “Translation Addition Theorems for Spherical Vector Wave Functions.” *Quart. Appl. Math.*, **20** 33–40 (1962)
12. Waterman, PC, “Symmetry, Unitary and Geometry in Electromagnetic Scattering.” *Phys. Rev. D*, **3** 825–839 (1971) doi:10.1103/PhysRevD.3.825
13. Mackowski, D, “Calculation of Total Cross Sections of Multiple-Sphere Clusters.” *J. Opt. Soc. Am. A*, **11** (11) 2851–2861 (1994)
14. Auger, JC, Stout, B, “A Recursive T-Matrix Algorithm to Solve the Multiple Scattering Equation: Numerical Validation.” *J. Quant Spectrosc. Radiat. Transfer.*, **79–80** 533–547 (2003) doi:10.1016/S0022-4073(02)00306-0
15. Quirantes, A, Arroyo, F, Quirantes-Ros, J, “Multiple Light Scattering by Spherical Particle Systems and Its Dependence on Concentration: A T-Matrix Study.” *J. Colloid Interf. Sci.*, **240** (1) 78–82 (2001) doi:10.1006/jcis.2001.7641
16. Vargas, WE, “Optical Properties of Pigmented Coatings Taking into Account Particle Interactions.” *J. Quant. Spectr. Radiat. Trans.*, **78** (2) 187–195 (2003)
17. Auger, JC, Stout, B, Martinez, V, “Scattering Efficiency of Aggregated Clusters of Spheres: Dependence on Configuration and Composition.” *JOSA A*, **22** 2700–2708 (2005)
18. “Standard Test Method for Hiding Power of Paints by Reflectometry.” *Book of ASTM Standards*, D2805–88.
19. Kubelka, P, Munk, F, “Ein Beitrag zur Optik der Farbanstriche.” *Z. Tech. Phys. (Leipzig)*, **12** 593–601 (1931)
20. Auger, JC, Martinez, V, Stout, B, “Absorption and Scattering Properties of Dense Ensemble of Nonspherical Particles.” *JOSA A*, **24** 3508–3351 (2007)
21. Hottel, HC, Sarofim, AF, Dalzell, WH, Vasalos, IA, “Optical Properties of Coatings, Effect of Pigment Concentration.” *AIAA J*, **9** (10) 1895–1898 (1970)